

Prediction of Crack Initiation in Combustion Chamber Liners

W.H. Vogel,* R.W. Soderquist,† and B.C. Schlein*
United Technologies, East Hartford, Conn.

An analytical procedure for predicting the crack initiation life of jet engine combustion chamber liners is presented. Sample calculations using the procedure are made and correlated against representative engine and test rig data. The analysis employs the Strain Range Partitioning Method, proposed by Manson et al., to determine the low cyclic thermal fatigue (LCTF) and creep damage components. A procedure for estimating plastic strain range and creep strain per cycle is presented, and life estimates are made using this in combination with a linear cumulative damage summation of the LCTF and creep damage components.

Nomenclature

a	=logarithmic slope of reversed plastic strain vs life curve
A, B, C	=constants in strain-life equations
b	=logarithmic slope of compressive creep strain reversed by plastic strain vs life curve
B_t	=time and temperature dependant proportionality constant in stress-strain equation
D_c	=creep ductility
D_p	=tensile ductility
E	=Young's modulus
K_1, K_2, K_3	=stress-strain proportionality constants, functions only of temperature
n	=logarithmic slope of stress-strain curve
N	=life, in cycles
q	=exponential decay constant in stress relaxation Eq. (6)
S	=stress
T	=temperature
$\Delta\epsilon$	=strain increment
ϵ	=strain
<i>Subscripts</i>	
c	=creep
e	=elastic conditions
i	=initial
p	=plastic
T	=total life
t	=function of time
cp	=tensile creep strain reversed by plastic strain conditions
pc	=compressive creep strain reversed by plastic strain conditions
pp	=reversed plastic strain conditions
t_4, t_5	=refers to compressor exit and turbine inlet gas temperatures
TR	=total range

Introduction

INCREASING demands for reduced costs, both in the design and development of new aircraft engines and in the maintenance and operation of current and new engine models, have underscored the pressing need for improved durability analysis techniques for hot section components. This paper

addresses this need in regard to the cracking mode of failure of combustion chamber liners.

Insofar as low cyclic thermal fatigue (LCTF) cracking is a primary mode of failure in combustion liners, the proposed analysis is an essential ingredient in the development of a comprehensive, mission-analysis-oriented, life-prediction system for gas turbine combustors. Such a system will improve combustor durability design capability, provide a method for defining realistic accelerated endurance tests which simulate design missions, and evaluate component life as a function of actual use in the field for maintenance and logistics purposes.

Background

Examples of typical combustion chamber liner failures are given in Figs. 1 and 2. The cracking shown in Fig. 1 is characteristic of LCTF failures in can-annular combustion chambers. Cracking initiates in the region of the seam weld-joggle radius and progresses circumferentially around the liner. The liner must be removed and repaired to prevent separation when such cracks are found in hot-section inspection. Figure 2 illustrates the typical cracking failure mode experienced in large-diameter annular combustion liners. In this case, cracking initiates either at the louver lip edge or sometimes in the seam weld and then progresses axially. As in the case of the can-annular liner, the burner must be removed and repaired before the axial crack reaches a critical length which fortunately, can be on the order of several inches.

Both of the cracking modes described are caused by cycling of the thermal gradient between the hot louver lip and the cold louver knuckle. This gradient results in a high hoop stress in the lip-seam weld area and a high bending stress in the seam weld-joggle radius area. The relative magnitudes of these bending and hoop stresses are dependent upon the liner radius. Smaller radius liners (can-annular burners) have bending stresses higher than hoop stresses, and hence failure is by circumferential cracking. Large radius liners (annular burners) have higher hoop stresses, and consequently fail by axial cracking. The relative magnitudes of hoop and bending stress components as a function of liner radius are given in Fig. 3.

Clearly, it is essential to have accurate knowledge of metal temperatures and gradients as a basis for calculating thermal stresses and strains for durability analysis. This is the subject of important parallel studies and development and will not be discussed here. For the purposes of this paper, it will be assumed that temperatures are known to sufficient accuracy by the user.

Application

The failure model proposed in this paper is being integrated into a comprehensive design system for the prediction of gas-

Presented as Paper 76-681 at the AIAA/SAE 12th Propulsion Conference, Palo Alto, Calif., July 26-29, 1976; submitted Aug. 20, 1976; revision received April 20, 1977.

Index category: Thermal Stresses.

*Assistant Project Engineer, Pratt and Whitney Aircraft Group, Commercial Products Division.

†Senior Analytical Engineer, Pratt and Whitney Aircraft Group, Commercial Products Division. Associate Fellow AIAA.

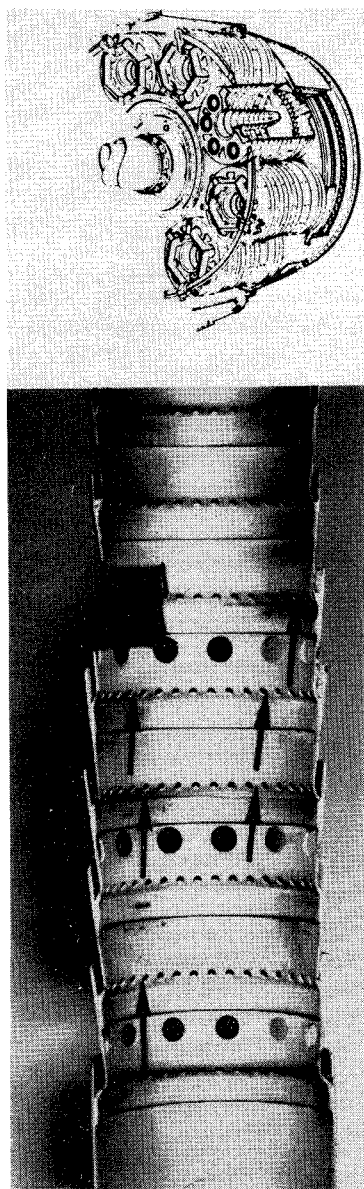


Fig. 1 Typical circumferential cracks in can-annular burner.

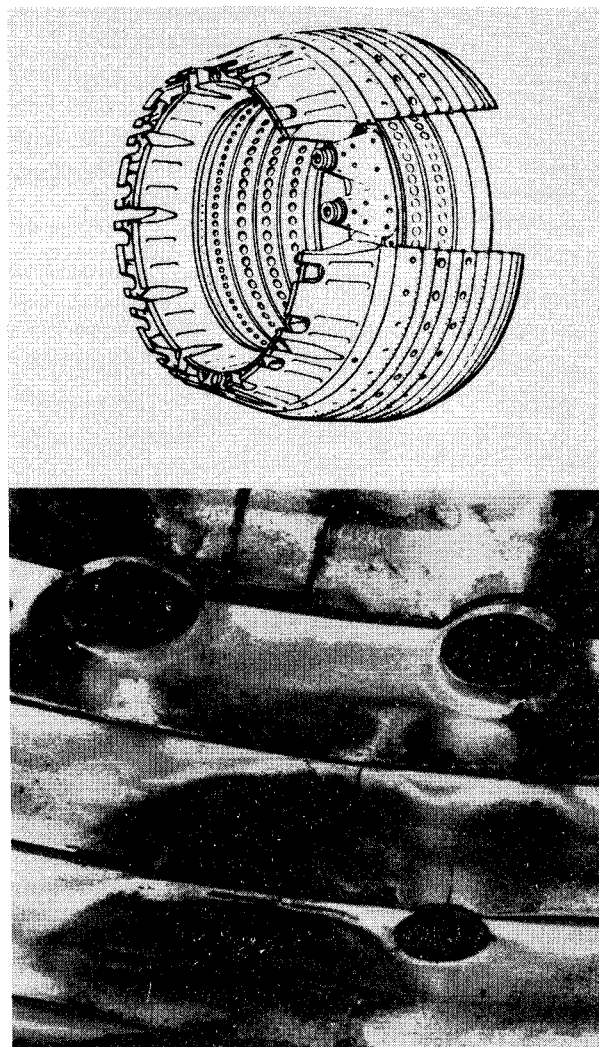


Fig. 2 Typical axial cracks in an annular liner.

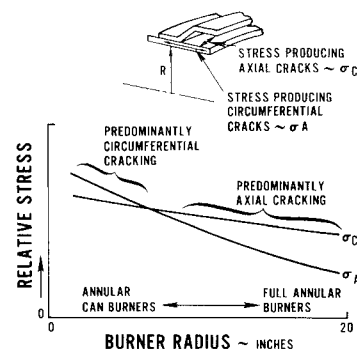
turbine engine combustion chamber life for particular applications and mission/route structures. An overview of the total design system envisioned is shown in the block diagram in Fig. 4. When completed, the resulting design system and mission analysis package will provide the capabilities already developed and in use for turbine blades at Pratt and Whitney Aircraft.¹

Some of these capabilities are: 1) improved design analysis capability and better initial design—reduced requirement for development testing, 2) capability to design accelerated engine endurance evaluation tests that faithfully simulate potential service application, 3) framework for evaluation of endurance test and service data, 4) basis for evaluation of alternate solutions to observed durability problems both in absolute durability benefit and cost effectiveness, and 5) maintenance and overhaul optimum scheduling for particular missions applications or route structures.

Damage Model Formulation

Air-cooled combustion chamber liners in general experience large thermally induced strains that exceed the elastic limits of the material at points of maximum stress and/or temperature. As pointed out previously, the most critical strains may be either hoop or bending strains depending upon the details of the specific configuration. Typical stress and temperature

Fig. 3 Relative magnitude of hood and bending stress components vs liner radius.



distributions will be illustrated for a conventional louvered liner construction but similar histories can be found in all air-cooled liner configurations to varying degrees.

Figure 5 illustrates the elastically calculated stress distribution in a louvered liner for the given typical temperature distribution. Parts A and B are liners with identical configuration and gradients except radius. Thus, as previously explained and as shown in Fig. 3, a small radius can-annular liner is bending stress limited at point 1, while the large radius annular liner is hoop stress limited at point 2. Although the elastically calculated stresses are in excess of the elastic limit at the critical locations, they are useful in estimating strain ranges. The total strain range is taken as the elastic stress divided by Young's modulus, S/E .

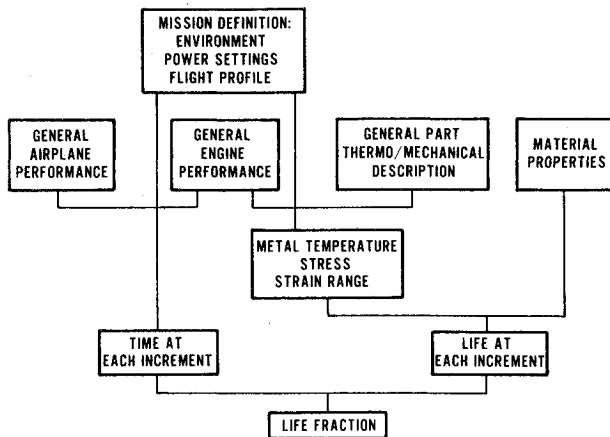


Fig. 4 Block diagram of mission analysis model.

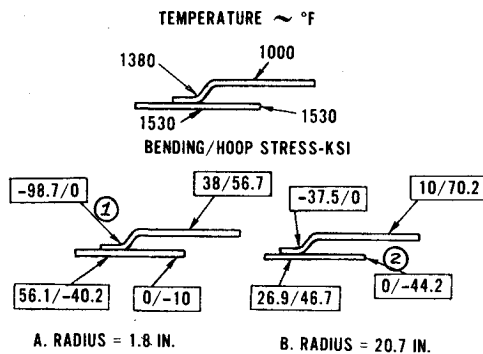


Fig. 5 Typical louver temperature and stress distribution.

Typically, a stress-strain hysteresis loop similar to that shown in Fig. 6 is assumed. The dwell representing time at takeoff, climb, and cruise conditions is hypothesized to result in a stress relaxation occurring essentially at constant strain. Following the lines of the Strain Range Partitioning Method proposed by Manson and his associates,² the inelastic strains occurring within the cycle are segregated into a time-independent component and a time-dependent (creep) strain component. The time-independent plastic strain component is taken as the plastic strain range that would occur if the reversal took place immediately without any dwell at the maximum strain condition. The time-dependent (creep) strain component is taken as the additional inelastic strain which occurs as a result of the dwell at maximum strain.

Using the definitions and notation of Manson,² the time-independent reversed plastic strain is called $\Delta\epsilon_{pc}$ and the fatigue damage associated with this component is hypothesized to be given by an expression of the form:

$$1/N_{pp} = (\Delta\epsilon_{pp}/AD_p)^{1/a} \quad (1)$$

In the Strain Range Partitioning Method² the damage associated with the time-dependent creep strain component depends on which mode of cracking is predominant.

In the case where the hoop stress, and consequently the axial mode of cracking is dominant, the creep damage component is of the $\Delta\epsilon_{pc}$ -type (i.e., compressive creep reversed by plastic strain) and is given by

$$1/N_{pc} = (\Delta\epsilon_{pc}/BD_p)^{1/b} \quad (2)$$

It is then assumed that the two forms of damage are linearly accumulative leading to the following relationships for the total life:

$$1/N_T = (1/N_{pp}) + (1/N_{pc}) \quad (3)$$

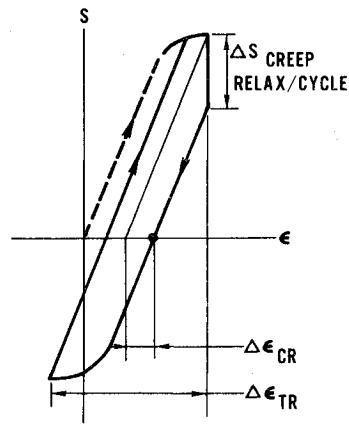


Fig. 6 Typical hysteresis loop.

Manson² uses an interaction damage rule rather than the linear model of Eq. (3), although he notes that there is little difference in the results.

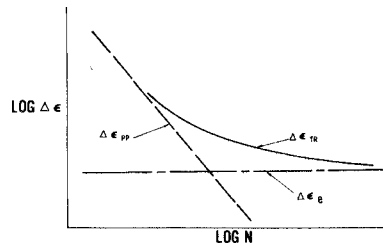
If the bending stress and therefore circumferential cracking mode is dominant, then the creep strain range component is defined as the type $\Delta\epsilon_{cp}$ (i.e., tensile creep strain reversed by compressive plastic strain) and the damage is given as

$$1/N_{cp} = (\Delta\epsilon_{cp}/CD_c)^{1/b} \quad (4)$$

Although the reverse component $\Delta\epsilon_{pc}$ is also present in bending, Manson concludes that the $\Delta\epsilon_{cp}$ cycle is generally more damaging for the same magnitude of strain range. This tends to be confirmed by the authors' experience that circumferential cracking begins on the side which is in tension at maximum temperature. However, in application to Hastelloy X burner liners, the authors have found that the recommended value of 0.25 for the proportionality constant is too low to correlate failure experience. Furthermore, it is found that the generally accepted level of creep or stress rupture ductility is also on the low side for correlation unless coefficients of A on the order of 2 or 3 are chosen. The best results, in the authors' problem, have been found using the same expression for the denominator as given by the theory for the $\Delta\epsilon_{pc}$ case (i.e., $1.25 D_p$). This is an important departure from the assumptions of Ref. 2 and as such bears further explanation than can be made at this time. The authors' speculation is that in their problem the creep strains are almost totally induced by stress relaxation, a large part of which is attributable to primary creep behavior. This may plausibly be more akin to short-time plastic strain damage than stress rupture damage, hence the better correlation with the tensile ductility D_p .

Determination of Time-Independent Plastic Strain Range— $\Delta\epsilon_{pp}$

Although the calculation of the cyclic plastic strains and strain ranges is a complex and difficult analytical task, it is felt by the authors that a reasonable estimate of $\Delta\epsilon_{pp}$ can be made using the following logic. The LCF strength of materials is commonly specified in curves showing the cycles to cracking as a function of the total strain range (elastic + plastic) on a log-log scale. These curves have the form shown in Fig. 7, and several models have been proposed in the literature for the relationship of the LCF curve to common materials properties, etc. The model proposed by Langer³ is particularly useful for our purposes. It envisions the curve to be formed by the sum of two components—1) a plastic strain range $\Delta\epsilon_{pp}$ vs N component and 2) an elastic strain range $\Delta\epsilon_e$ component, taken as two lines on the log-log plot in Fig. 7. Using this model, it is then reasoned that the plastic strain range can be back calculated by subtracting the

Fig. 7 Log $\Delta\epsilon$ vs log N with Langers hypothesis.

elastic strain range from the total strain range:

$$\Delta\epsilon_{pp} = \Delta\epsilon_{TR} - \Delta\epsilon_e \quad (5)$$

Equation 5 provides a simple estimate of plastic strain range, requiring only the total strain range as calculated by elastic analysis and the value of $\Delta\epsilon_e$ as estimated from the conventional endurance limit or curve fit for actual LCF data.

Determination of Time-Dependent

Strain Range— $\Delta\epsilon_{pc}$ or $\Delta\epsilon_{cp}$

In general, the stresses/strains causing failure in combustion liners are the direct result of thermal growth incompatibilities and as such come under the class of strain-controlled cyclic problems. It is therefore postulated that the creep strains induced during a typical cycle are primarily the result of stress relaxation at constant total strain. Referring to Fig. 6, the creep strain associated with a given stress relaxation is taken as the change in elastic strain or simply as $\Delta S/E$.

Several alternative approaches can be taken in the calculation of the stress relaxation occurring in the cycle. For the sake of convenience, it was deemed desirable to use a closed-form solution rather than an iterative solution approach. Such a solution is, therefore, proposed in the following description.

A relationship between creep, stress, and time as given by Marin⁴ is assumed:

$$\epsilon = [K_1 + K_2(1 - e^{-qt}) + K_3t] S^n \quad (6)$$

The first term in the parentheses is proportional to the initial loading strain, the second term to the transient creep strain, and the third term to the steady-state creep term. Insofar as the expression within the parentheses is a function of temperature only, for a given material Eq. 6 can be simplified to

$$\epsilon = B_1 S^n \quad (7)$$

Now, recalling our previous postulate that the process to be defined is primarily a constant strain, stress relaxation, it is stated that the total strain remains constant at its initial value throughout the relaxation interval. Therefore,

$$B_1 S^n = \epsilon_i = K_1 S_i^n \quad (8)$$

which can be restated to give

$$S_i - S = S_i [1 - (K_1/B_1)^{1/n}] \quad (9)$$

and then dividing by Young's modulus to convert the stress terms to strain terms,

$$\Delta\epsilon_{pc} \text{ or } \Delta\epsilon_{cp} = \left(\frac{\epsilon_{TR}}{K_1}\right)^{1/n} \frac{10^3}{E} \left[1 - \left(\frac{K_1}{B_1}\right)^{1/n}\right] \quad (10)$$

in which the initial strain ϵ_i is replaced by its equivalent, the total strain as calculated by elastic analysis.

Thus, a relatively easy-to-use expression for estimating the creep strain component of cyclic plastic strain in terms of

Fig. 8 Graphical illustration of the time hardening theory.

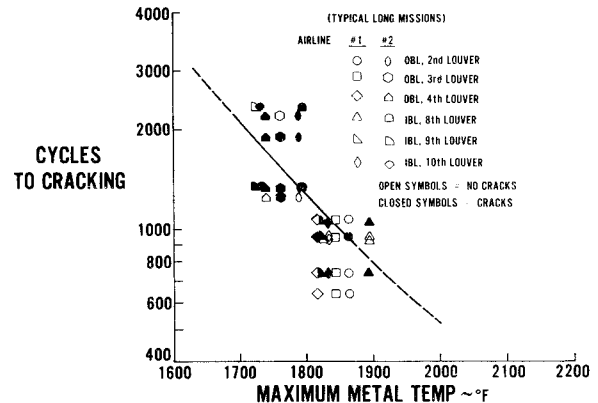
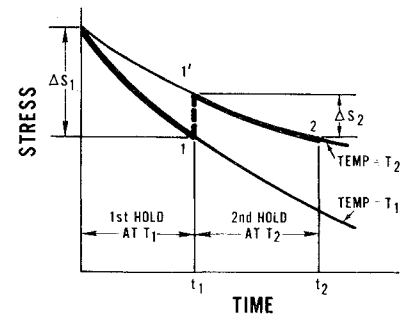


Fig. 9 Correlation of annular burner creep—LCTF model.

materials parameters that can readily be determined from conventionally available mechanical properties has been derived and is used in this analysis.

Creep Relaxation under Varying Hold Conditions

A typical aircraft mission cycle involves hold periods at various power conditions and therefore at varying temperature levels. This raises the question of how one applies Eq. 10 to multiple hold conditions. Of the alternative approaches generally used for cumulative creep calculations, the most applicable to this problem would appear to be either the Strain Hardening Theory or the Time Hardening Theory approach.⁵ Although either of these theories can be applied to the required calculation, it is more convenient to use the time hardening theory in our case because it can be formulated explicitly. Consequently, it is this approach that will be used in the model formulation subject to later review if required.

The concept of the time hardening theory is illustrated graphically in Fig. 8. Basically, the stress relaxation for each incremental hold period (e.g., sea-level takeoff, climb, cruise, etc.) is calculated as the relaxation that occurs between the initial and final time limits of the particular hold at the respective temperature. Mathematically this is expressed as follows:

$$(\Delta\epsilon_{CR})_i = (\Delta\epsilon_{CR})_{t_i} - (\Delta\epsilon_{CR})_{t_{i-1}} \quad (11)$$

where Eq. 10 is used to find the terms on the right-hand side of the equation.

Correlation of Predictions with Data

The proposed system is currently undergoing evaluation as a design tool at Pratt and Whitney Aircraft as part of an Air Force contract.⁶ Although the correlation process is not yet finished, early results are very encouraging and are worth presenting. Basically, there are two classes of problems of particular interest for correlation: large-diameter annular burners with axial cracking failure mode, and small-diameter can-annular burners with circumferential cracking failure modes.

Table 1 Sample creep—LCFT mission life calculation, Hastelloy X can-annular burner^a

Flight condition	t_{incr} , sec	T_{15} , °F	T_{14} , °F	T_{metal} , °F	T_{metal} , °F	ϵ^{TR} %	$E \times 10^{-6}$, psi	$k_I \times 10^6$	%	D_p , %	$B_i(i-1) \times 10^6$	$B_i i \times 10^6$
Takeoff	70	2106	884	1546	496	.581	20.5	1.7	.180	45	1.7	4.5
Avg. Climb	720	1867	767	1392	22.0	1.4	...	54	1.4	2.2
Avg. Cruise	2160	1656	651	1231	T_m below normal creep range: assume negligible creep damage					
Flight condition	CR_{incr} , %	Incremental creep damage			$\Delta \epsilon_p$, %	LCTF damage	Total damage	N_T , cycles				
Takeoff	.0525	.000163			.041	.000618	.000781	...				
Avg. climb	.0274	.0000721		0000721	...				
Avg. cruise	neg.	neg.						
Totals000235		000618	.00853	1172				

^a Given conditions and corresponding materials properties: $n = 2.35$, $a = 0.6$, $b = 0.8$.

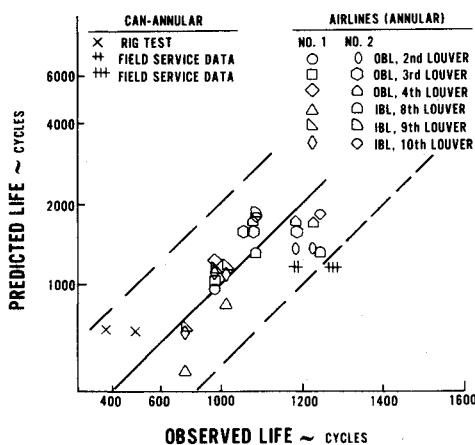


Fig. 10 Comparison of creep—LCTF life prediction with field service experience.

Figure 9 shows data taken from damage surveys conducted on annular liners in service with two different airlines. The critical regions in this combustion chamber are found in the front end of the outer liner and the aft end of the inner liner. The plotted symbols indicate results of inspections of various engines at different times. Open symbols indicate that no cracking distress was observed at inspection. The individual points are plotted at the estimated maximum metal temperature for the particular louver and the particular application. These temperature estimates were derived from analysis calibrated with thermocouple temperature measurements made in experimental engines.

The curve drawn in the preceding plot represents the typical mission life predicted by the creep LCTF analysis proposed in this paper. Mission life is given in number of flights or missions and is calculated from the linear accumulation of damage at the sea-level takeoff, climb, cruise, and thrust reverse operating points as illustrated in the sample calculation in Table 1. Considering the complexity of the problem, it is concluded that the correlation obtained is quite good, especially if it is found to be repeatable in varying applications (e.g., long-range vs short-range missions, different engines, experimental engine tests, etc.).

Application of the analysis to a typical can-annular problem is demonstrated in the correlation of predicted vs observed life in Fig. 10. In this case, the data are taken from a rig test of a section of the burner in which the louver lip is alternately heated and cooled between 1600°F and room temperature. Also shown in this figure is the observed life in

this mode of failure of the particular configuration tested in airline service and the corresponding correlations of the cracking data for the axial cracking mode for annular liners taken from Fig. 9. It can be seen from Fig. 10 that almost all of the points fall within a factor of 2 of the 1:1 correlation line. This is within the accuracy of the Strain Range Partitioning Method correlation with laboratory data claimed by Manson.²

Conclusions

Based on the correlations obtained and shown in Figs. 9 and 10, the authors conclude that the strain range partitioning approach combined with the stress/strain calculation procedure proposed in this paper is indeed a viable method for the prediction of combustion chamber liner life to a cracking mode of failure. The model as presented predicts life to crack initiation and as such is not the complete answer on total useful life of the liner before removal is required. Further studies are required either to correlate the rate of progression to failure by fracture mechanics theory or by data correlation techniques. Finally, it should be appreciated that accurate knowledge of the metal temperatures and gradients are a vital part of the application of this theory. The potential user should, therefore, be just as careful in determining this input required for life prediction.

Acknowledgment

This work was developed under Air Force Contract F33615-75-C-2057, "Reliability Prediction for Combustors and Turbines," Air Force Aero Propulsion Laboratory, Wright-Patterson Air Force Base, Ohio.

References

- ¹ Loferski, M.T., "Turbine Airfoil Life Prediction by Mission Analysis," *Journal of Aircraft*, Vol. 12, April 1975, pp. 400-402.
- ² Manson, S.S., "The Challenge to Unify Treatment of High Temperature Fatigue—A Partisan Proposal Based on Strainrange Partitioning," *Fatigue at Elevated Temperatures*, American Society for Testing and Materials, ASTM STP 520, 1973, pp. 744-782.
- ³ Langer, B.F., "Design of Pressure Vessels for Low Cycle Fatigue," *Journal of Basic Engineering, Transactions of ASME*, Ser. D, Vol 84, Sept. 1962, p. 389.
- ⁴ Marin, J., *Mechanical Behavior of Engineering Materials*, Prentice-Hall, Inc., Englewood Cliffs, N.J., 1962.
- ⁵ Mendelson, A., Hirschberg, M.H., and Manson, S.S., "A General Approach to the Practical Solution of Creep Problems," *Journal of Basic Engineering*, Vol. 81, Dec. 1959, pp. 585-598.
- ⁶ "Reliability Prediction for Combustor and Turbines," Air Force Aero Propulsion Laboratory, Air Force Systems Command, United States Air Force, Wright Patterson Air Force Base, Ohio, Contract No. F-33615-75-C-2057, June 25, 1975.